

## Orthorhombic-to-tetragonal transition in $R_{1+x}\text{Ba}_{2-x}\text{Cu}_3\text{O}_{7+\delta}$ ( $R = \text{Nd, Sm, and Eu}$ )

S. Li, E. A. Hayri, K. V. Ramanujachary, and Martha Greenblatt\*

*Department of Chemistry, Rutgers-The State University, New Brunswick, New Jersey 08903*

(Received 14 March 1988; revised manuscript received 23 May 1988)

The orthorhombic-to-tetragonal structural phase transition in the high- $T_c$  superconducting oxides of the type  $R_{1+x}\text{Ba}_{2-x}\text{Cu}_3\text{O}_{7+\delta}$  [ $R$  (for rare earth) = Nd, Sm, and Eu] has been investigated using powder x-ray diffraction, dc resistivity, and thermogravimetric techniques. It was found that the orthorhombic-to-tetragonal transition occurs for samples whose nominal stoichiometric content of oxygen is greater than 7.0 ( $0 < \delta < 0.3$ ) as compared to less than 7.0 in  $\text{YBa}_2\text{Cu}_3\text{O}_{7-\delta}$ . With increasing  $[R/\text{Ba}]$  ratio in  $R_{1+x}\text{Ba}_{2-x}\text{Cu}_3\text{O}_{7+\delta}$ , a clear convergence of multiple orthorhombic peaks to a well-defined single tetragonal peak was observed in the x-ray diffraction pattern. The presence of orthorhombic distortion in this system appears to be essential for achieving 90-K superconductivity.

### INTRODUCTION

It is well established that the high- $T_c$  superconducting oxides  $R\text{Ba}_2\text{Cu}_3\text{O}_{7-\delta}$  (referred to as 1:2:3 compounds, where  $R = \text{Y}$  and all the rare-earth elements except Ce, Pr, and Tb) undergo an orthorhombic-to-tetragonal transition as a result of variation in the oxygen content and oxygen distribution.  $T_c$  is dramatically effected by oxygen content, oxygen distribution, and crystal symmetry.<sup>1,2</sup> For  $\delta = 0$ , the crystal symmetry is orthorhombic and  $T_c \sim 92$  K. When samples are heat treated at elevated temperatures and/or in reducing atmospheres, the oxygen content and  $T_c$  decrease; at  $\delta > 0.5$ , the samples may be tetragonal and semiconducting. The depletion of the oxygen content of 1:2:3 compounds also leads to the reduction of both the formal oxidation state and coordination number of the Cu(1) atoms in the Cu-O one-dimensional chains along the  $b$  direction. In the fully oxygenated orthorhombic form of 1:2:3, the average formal valence of copper is 2.33 and all of the O(4) ( $0, \frac{1}{2}, 0$ ) positions are occupied, while all of the O(5) ( $\frac{1}{2}, 0, 0$ ) positions are empty.<sup>3</sup> In tetragonal  $\text{YBa}_2\text{Cu}_3\text{O}_6$ , Cu(1) appears to have a formal charge of +1 and twofold coordination to oxygen along the  $c$  axis of the unit cell.<sup>4</sup> The tetragonal form of 1:2:3 is semiconducting, while the ordered orthorhombic  $\text{YBa}_2\text{Cu}_3\text{O}_{6.3}$  is superconducting;<sup>5,6</sup> in the former, the O(4) and O(5) positions are randomly occupied, in the latter, although a large number of O(4) atoms are missing along the  $b$  axis, the long-range order of the Cu-O chain is maintained.  $\text{YBa}_2\text{Cu}_3\text{O}_{7-\delta}$  with  $0.3 < \delta < 0.5$  prepared at low temperature by oxygen getter methods is a  $\sim 60$ -K bulk superconductor.<sup>2,5</sup> Thus, both oxygen content and the microscopic oxygen configuration has a large effect on  $T_c$ , and near full ( $\delta < 0.2$ ) occupation of the O(4) positions is required for 90-K superconductivity. The structural and transport properties of orthorhombic and tetragonal  $\text{YBa}_2\text{Cu}_3\text{O}_{7-\delta}$  phases are well established.

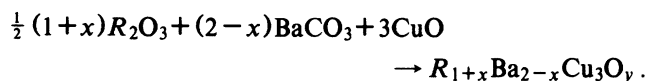
In addition to thermal treatments, the oxygen content and the crystal symmetry of the 1:2:3 compounds may be changed by chemical substitution. For example, in

$\text{La}_{1+x}\text{Ba}_{2-x}\text{Cu}_3\text{O}_{7+\delta}$ ,  $\text{La}^{3+}$  substitution for  $\text{Ba}^{2+}$  leads to an increase in the oxygen content, a change in the distribution of oxygen ions in the lattice, and concomitant changes in crystal symmetry, electronic properties, and  $T_c$ .<sup>6,7</sup> For  $0 < x < 0.3$  the samples are orthorhombic and superconducting, while for  $x > 0.3$ , the samples are tetragonal and semiconducting.  $\delta$  increases with increasing  $x$ ; however, the formal oxidation state of copper is 2.33, nearly independent of the oxygen content.<sup>6</sup> This suggests that the copper oxidation state alone is not sufficient to produce superconductivity. More recent reports indicated that even small rare-earth ions including Nd, Sm, Eu, and Y can substitute for the large Ba cations in the 1:2:3 structure leading to higher oxygen content than seven.<sup>8-10</sup> However, in these reports, the relationship between the oxygen content, orthorhombic-to-tetragonal phase transformation, and superconducting behavior was not established in detail. Substitutions for Cu by all of the 3d transition-metal cations or by  $\text{Al}^{3+}$  or  $\text{Ga}^{3+}$  have also been carried out; some of these substitutions also lead to orthorhombic-to-tetragonal phase transitions. Nevertheless, it is not clear at the present what the effect of 3d transition metal or that of the  $\text{Al}^{3+}$  or  $\text{Ga}^{3+}$  ion substitutions are on the oxygen content or oxygen ordering of the 1:2:3 compounds.<sup>11-13</sup>

We have undertaken a systematic investigation of  $R(\text{Ba}_{2-x}\text{R}_x)\text{Cu}_3\text{O}_{7+\delta}$  with  $R = \text{Nd, Sm, and Eu}$  in order (i) to examine the range of  $x$  for solid solution formation and its relationship to oxygen content, copper valence, and high- $T_c$  superconductivity; (ii) to find unambiguous evidence of orthorhombic-to-tetragonal transition in these substituted phases and to establish the relationship between oxygen content and symmetry transformation. In this Communication, we show an upper limit of oxygen content for the existence of the high- $T_c$  superconducting phase and unambiguous evidence of orthorhombic-to-tetragonal transition in  $R(\text{Ba}_{2-x}\text{R}_x)\text{Cu}_3\text{O}_{7+\delta}$  with  $R = \text{Nd, Sm, and Eu}$ ; the transition is sharp and occurs at  $x \approx 0.2$ . The oxygen content increases, while  $T_c$  decreases with increasing  $x$ .

## EXPERIMENT

Rare-earth oxides used in this investigation were fired at 950°C in air to eliminate hydrates, carbonates, and other impurity adsorbates. Stoichiometric amounts of reagent grade, or better purity Nd<sub>2</sub>O<sub>3</sub> or Sm<sub>2</sub>O<sub>3</sub>, or Eu<sub>2</sub>O<sub>3</sub>, BaCO<sub>3</sub>, and CuO were weighed according to the chemical equation



The mixtures were ground in an agate mortar and calcined in air of 950°C with repeated grindings and refirings (usually two or three), until no changes in the powder x-ray diffraction could be detected. The powder samples were pressed into pellets and then sintered at 950°C for 24 hs. In order to maximize the oxygen content, pellet samples were annealed at 450–500°C in flowing oxygen atmosphere for 24 h, followed by slow cooling to room temperature. X-ray powder diffraction data were recorded by a SCINTAG PAD IV diffractometer using Si as an internal standard. Oxygen contents were determined by H<sub>2</sub> reduction of the powder specimens in a DuPont 951 thermogravimetric analyzer (TGA). Electrical resistivity was measured in the temperature range 4–300 K on rectangularly shaped bar samples with indium solder contacts in a four-probe configuration. All measurements reported in this investigation are reproducible.

## RESULTS AND DISCUSSION

X-ray powder diffraction data indicate that the solubility limit of  $R(Ba_{2-x}R_x)Cu_3O_{7+\delta}$  with  $R = Nd, Sm,$  and  $Eu$  is  $0 \leq x \leq 0.5$ . The prediction of Zhang *et al.*,<sup>9</sup> of a larger upper limit of solubility in  $R(Ba_{2-x}R_x)Cu_3O_{7+\delta}$  with increasing size of the rare-earth ion was not observed. For compositions corresponding to  $x = 0.5$  the powder x-ray diffraction patterns of  $R(Ba_{2-x}R_x)Cu_3O_{7+\delta}$  analogs show close resemblance to that of  $La_3Ba_3Cu_6O_{14+\delta}$  (3:3:6). Figure 1 compares the diffraction patterns of  $Nd(Ba_{2-x}Nd_x)Cu_3O_{7+\delta}$  of  $x = 0.0$  and  $x = 0.5$ . It is evident that the 3:3:6 analogs of Sm, Nd, and Eu are isostructural with their parent 1:2:3 structures in agreement with recent neutron and x-ray diffraction studies of  $Nd_{1+x}Ba_{2-x}Cu_3O_y$ .<sup>14,15</sup> At  $x > 0.5$  decomposition of the perovskite-type phase occurs, and an impurity phase of  $K_2NiF_4$ -type shows up in the powder-diffraction patterns of Sm and Eu at  $x = 0.6$ ; an unidentified phase is seen in the Nd system at  $x = 0.6$ .

Table I summarizes the unit-cell parameters, crystal symmetry, total oxygen content, and  $T_c$  for the series  $R(Ba_{2-x}R_x)Cu_3O_{7+\delta}$  ( $R = Nd, Sm,$  and  $Eu$ ). Cell parameters were determined by fitting the observed x-ray data by least-squares refinement techniques. Orthorhombic  $Nd(Ba_{2-x}Nd_x)Cu_3O_{7+\delta}$ ,  $Sm(Ba_{2-x}Sm_x)O_{7+\delta}$ , and  $Eu(Ba_{2-x}Eu_x)Cu_3O_{7+\delta}$  show a decrease in the  $b$  and  $c$  cell parameters, and an increase in the  $a$  parameter with increasing  $[R]/[Ba]$  ratio.  $a$  and  $b$  converge for  $x \approx 0.2$  (Fig. 2), then decrease monotonically. Thus, the orthorhombic-to-tetragonal phase transition is clearly

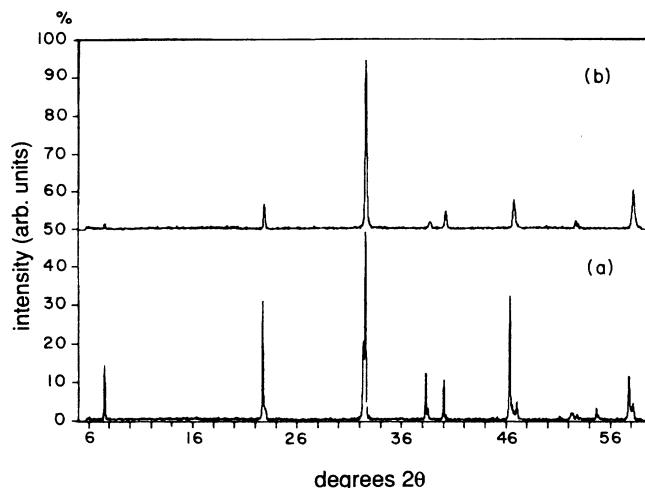


FIG. 1. Comparison of powder x-ray-diffraction patterns of two members of the solid solution series  $Nd_{1+x}Ba_{2-x}Cu_3O_{7+\delta}$  (a)  $x = 0.0$ ; (b)  $x = 0.5$  (Nd 3:3:6).

resolved in all three systems. Peak profiles of the (006), (020), and (200) reflections as a function of  $x$  in  $Nd(Ba_{2-x}Nd_x)Cu_3O_{7+\delta}$  are presented in Fig. 3. For  $x = 0$ , the characteristic orthorhombic splitting of the peak is seen. With increasing  $x$ , the triplet peak gradually transforms first to a doublet and eventually to a single peak at  $x = 0.5$ . Similar behavior is seen in the Sm and Eu analogs, except that the tetragonal phase seems to be stabilized for smaller values of  $x$  ( $\sim 0.1$ – $0.2$ ).

Figure 4 shows the variation of the total oxygen content in  $Nd(Ba_{2-x}Nd_x)Cu_3O_{7+\delta}$  as a function of  $x$  as determined by thermogravimetric analysis (TGA). A nearly monotonic increase in  $\delta$  with increasing  $x$  is observed. In all three systems, we see a clear transition from orthorhombic-to-tetragonal symmetry at  $\delta = 0.10 \pm 0.01$ . This indicates that a minimum occupancy of the O(5) site is required to increase the symmetry. At low values of  $\delta$ , all of the O(4) sites, and few of the O(5) sites are occupied so that orthorhombic symmetry and long-range order of the one-dimensional  $Cu-O$  chains in the  $b$  direction remain,

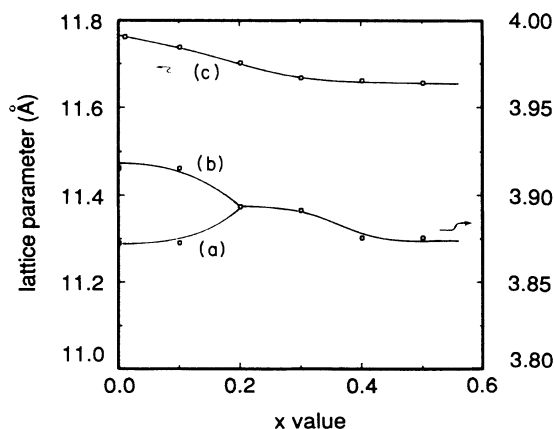


FIG. 2. Variation of the cell parameters  $a$ ,  $b$ , and  $c$  as a function of  $x$  in  $Nd_{1+x}Ba_{2-x}Cu_3O_{7+\delta}$ .

TABLE I. Physical parameters of  $R_{1+x}\text{Ba}_{2-x}\text{Cu}_3\text{O}_{7+\delta}$ ,  $R=\text{Nd, Sm, and Eu}$ . In the crystal symmetry column,  $O$  and  $T$  denote orthorhombic and tetragonal, respectively.

Composition $x$	Crystal symmetry	Cell parameters ( $\text{\AA}$ )			$T_c^{\text{onset}}$ (K)	$T_c^{\text{zero}}$ (K)	$\delta$
		$a$	$b$	$c$			
<b><math>\text{Nd}_{1+x}\text{Ba}_{2-x}\text{Cu}_3\text{O}_{7+\delta}</math></b>							
0.0	$O$	3.871(2)	3.914(1)	11.756(2)	88	77	0.04
0.1	$O$	3.871(1)	3.914(3)	11.7321(1)	81	50	0.05
0.2	$T$	3.890(1)	3.892(2)	11.696(2)	54	33	0.10
0.3	$T$	3.890(2)	...	11.661(1)	50	14	0.14
0.4	$T$	3.874(3)	...	11.659(4)	...	...	0.19
0.5	$T$	3.876(3)	...	11.649(1)	...	...	0.30
<b><math>\text{Sm}_{1+x}\text{Ba}_{2-x}\text{Cu}_3\text{O}_{7+\delta}</math></b>							
0.0	$O$	3.858(0)	3.910(0)	11.741(0)	92	82	0.01
0.1	$O$	3.860(2)	3.906(2)	11.729(3)	87	70	0.05
0.2	$T$	3.881(0)	...	11.654(2)	47	29	0.09
0.3	$T$	3.879(2)	...	11.630(2)	...	...	0.16
0.4	$T$	3.871(1)	...	11.599(2)	...	...	0.19
0.5	$T$	3.861(2)	...	11.603(3)	...	...	0.22
<b><math>\text{Eu}_{1+x}\text{Ba}_{2-x}\text{Cu}_3\text{O}_{7+\delta}</math></b>							
0.0	$O$	3.844(1)	3.904(4)	11.709(4)	92	88	0.01
0.1	$O$	3.854(3)	3.887(8)	11.679(6)	92	70	0.07
0.2	$T$	3.873(0)	...	11.631(2)	56	28	0.18
0.3	$T$	3.867(1)	...	11.624(2)	53	26	0.15
0.4	$T$	3.873(3)	...	11.619(2)	43	13	0.16
0.5	$T$	3.859(1)	...	11.579(3)	...	...	0.32

mediating superconductivity. However, at higher values of  $\delta$  with more of the O(5) sites being occupied, the structural transformation to tetragonal symmetry occurs; the chains are partially replaced by Cu–O octahedral layers in the basal plane ( $ab$ ) and superconductivity is destroyed. A recent report suggests that by annealing the 3:3:6 samples under high oxygen pressure, the O(5) occupancy might be increased up to  $\delta=0.6$  with superconduc-

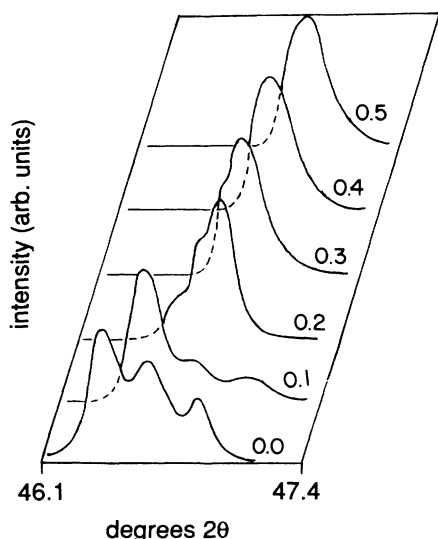


FIG. 3. X-ray-diffraction peak profiles of the (200), (006), and (020) reflections of  $\text{Nd}_{1+x}\text{Ba}_{2-x}\text{Cu}_3\text{O}_{7+\delta}$  as a function of  $x$ .

tivity observed in the sample at  $\sim 30$  K.<sup>16</sup> However, this result needs to be confirmed by others.

The temperature dependence of resistivity is shown in Fig. 5 for  $R(\text{Ba}_{2-x}\text{R}_x)\text{Cu}_3\text{O}_{7+\delta}$  with  $R=\text{Nd, Sm}$  for the range  $0 \leq x \leq 0.5$ . For  $x=0$  ( $\delta=0$ ), metallic behavior between 300–90 K and a metal-to-superconductor transition at 90 K are observed. The room-temperature resistivity values scale linearly with  $x$ . A local minima is evident before the onset of superconductivity for compositions with  $0.2 < x < 0.4$  for Nd and with  $0.1 < x < 0.3$  for

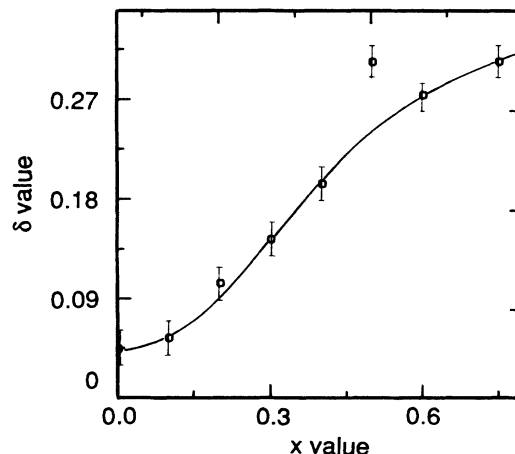


FIG. 4. The oxygen content  $\delta$  as a function of  $x$  in  $\text{Nd}_{1+x}\text{Ba}_{2-x}\text{Cu}_3\text{O}_{7+\delta}$ .

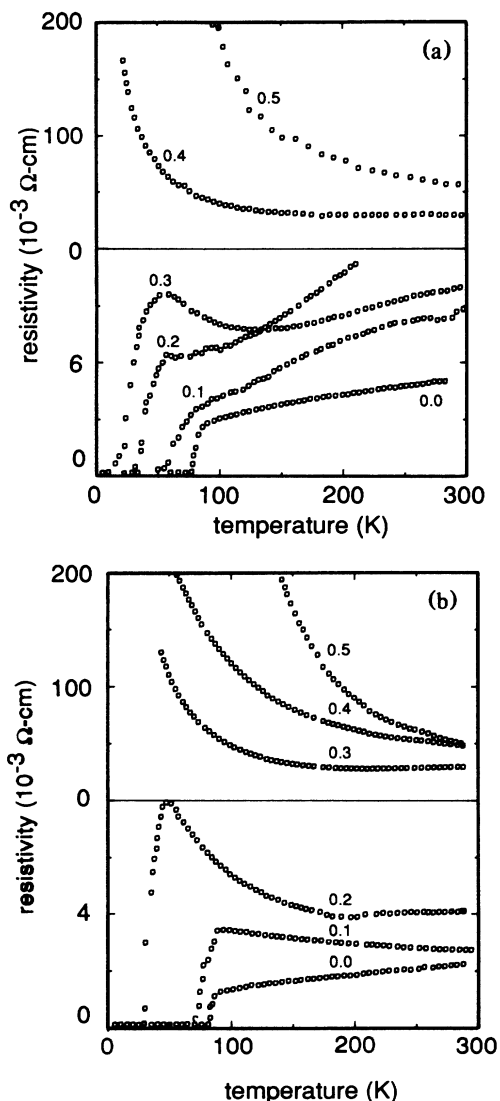


FIG. 5. Temperature dependence of the resistivity as a function of temperature in  $R_{1+x}\text{Ba}_{2-x}\text{Cu}_3\text{O}_{7+\delta}$ . (a)  $R=\text{Nd}$ ; (b)  $R=\text{Sm}$ .

the Sm compounds. Figure 6 indicates the variation of  $T_c$  with  $x$  for the Nd and Sm series of solid solutions.  $T_c$  decreases with increasing  $x$  for both in a similar way. When  $x \geq 0.4$  for the Nd and  $x \geq 0.3$  for the Sm series, only semiconducting behavior is seen down to 4 K. The Eu compound is still superconducting at  $x=0.4$  at low temperature (Table I). These results indicate that the tetragonal phase has a deleterious effect on the superconducting properties in these systems providing further evidence that square planar coordination of Cu(1) in the  $bc$  plane is essential for superconductivity. The metal-to-semiconductor transition and the broadening of the superconducting transition seen in some of the substituted samples (Fig. 5) are attributed to inhomogeneities of the samples.

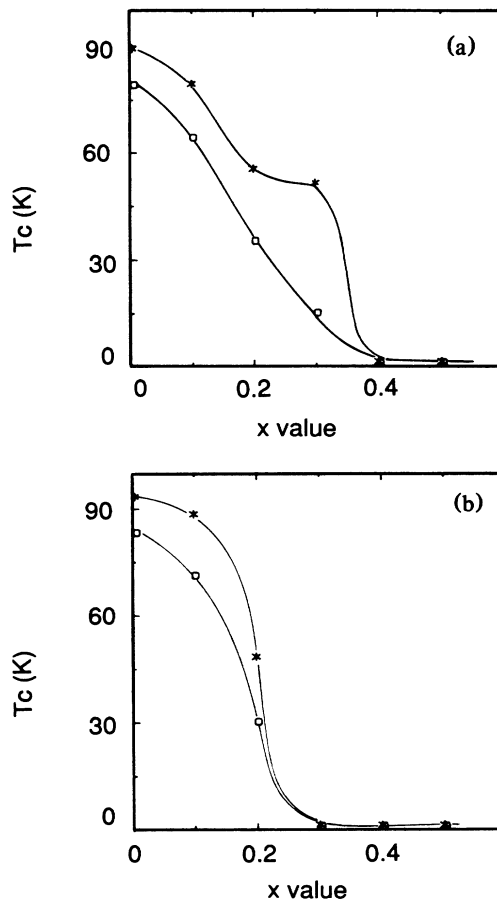


FIG. 6.  $T_c$  as function of  $x$  in the solid solution series (a)  $\text{Nd}_{1+x}\text{Ba}_{2-x}\text{Cu}_3\text{O}_{7+\delta}$ , and (b)  $\text{Sm}_{1+x}\text{Ba}_{2-x}\text{Cu}_3\text{O}_{7+\delta}$ . \*,  $T_c^{\text{onset}}$ ;  $\square$ ,  $T_c^{\text{zero}}$ .

Part of the inhomogeneities might be due to differences in the relative occupancy of the O(4) and O(5) sites in different regions of the pellet specimen. However, it might be partly due the magnetic rare-earth ions (Nd, Sm, Eu) on the  $\text{Ba}^{2+}$  site effecting superconductivity.

In summary, we have found solid solution formation in  $R_{1+x}\text{Ba}_{2-x}\text{Cu}_3\text{O}_{7+\delta}$  ( $R=\text{Nd}$ , Sm, and Eu) for  $0 \leq x \leq 0.5$ . With increasing  $x$ , the oxygen content increases and the formal oxidation state of Cu remains  $\sim 2.33$ . A clear orthorhombic-to-tetragonal phase transition at  $x \sim 0.2$  is observed.  $T_c$  decreases with increasing oxygen content.

#### ACKNOWLEDGMENTS

We wish to acknowledge helpful discussions with Dr. S. Fine. This work was supported by the Office of Naval Research and by the National Science Foundation Solid State Chemistry Grants No. DMR-84-04003 and No. DMR-87-14072.

- \* Author to whom communications should be addressed.
- <sup>1</sup>J. D. Jorgensen, B. W. Veal, W. K. Kwok, G. W. Crabtree, A. Umezawa, L. J. Nowicki, and A. P. Palikas, *Phys. Rev. B* **36**, 5731 (1987).
- <sup>2</sup>R. J. Cava, B. Batlogg, C. M. Chen, E. A. Rietman, S. M. Zahurak, and D. Werder, *Nature* **329**, 423 (1987).
- <sup>3</sup>P. K. Gallagher, M. M. O'Bryan, S. A. Sunshine, and D. W. Murphy, *Mater. Res. Bull.* **22**, 995 (1987).
- <sup>4</sup>A. Santoro, S. Miraglia, F. Beech, S. A. Sunshine, D. W. Murphy, L. F. Schneemeyer, and J. V. Waszczak, *Mater. Res. Bull.* **22**, 1007 (1987).
- <sup>5</sup>J. Cava, B. Batlogg, C. H. Chen, E. A. Rietman, S. M. Zahurak, and D. Werder, *Phys. Rev. B* **36**, 5719 (1987).
- <sup>6</sup>C. U. Segre, B. Dabrowski, D. G. Hinks, K. Zhang, J. D. Jorgensen, M. A. Beno, and I. K. Schuller, *Nature* **329**, 227 (1987).
- <sup>7</sup>S. A. Sunshine, L. F. Schneemeyer, J. V. Waszczak, D. W. Murphy, S. Miraglia, A. Santoro, and F. Beech, *J. Cryst. Growth* **85**, 632 (1987).
- <sup>8</sup>Z. Iqbal, F. Reidinger, A. Bose, N. Cipollini, T. J. Talor, H. Eckhardt, B. L. Ramakrishna, and E. W. Ong, *Nature* **331**, 326 (1988).
- <sup>9</sup>K. Zhang, B. Dabrowski, C. U. Segre, D. G. Hinks, I. K. Schuller, J. D. Jorgensen, and M. Slaski, *J. Phys. C* **20**, L935 (1987).
- <sup>10</sup>T. Iwata, M. Hikita, Y. Tajima, and S. Tsurumi, *Jpn. J. Appl. Phys. Lett.* **26**, L2049 (1987).
- <sup>11</sup>Y. Maeno, M. Kato, Y. Aoki, and T. Fujita, *Jpn. J. Appl. Phys. Lett.* **26**, L1982 (1987).
- <sup>12</sup>T. Siegrist, L. F. Schneemeyer, J. V. Waszczak, N. P. Singh, R. L. Opila, B. Battlog, L. W. Rupp, and D. W. Murphy, *Phys. Rev. B* **36**, 8365 (1987).
- <sup>13</sup>I. Sankawa, M. Sato, and T. Konaka, *Jpn. J. Appl. Phys. Lett.* **26**, L1616 (1987).
- <sup>14</sup>F. Izumi, S. Takekawa, Y. Matsui, N. Iyi, H. Asano, T. Ishi, and N. Watanabe, *Jpn. J. Appl. Phys.* **26**, L1616 (1987).
- <sup>15</sup>K. Takita, H. Katoh, H. Akinaga, M. Nishino, T. Ishigaki, and H. Asano, *Jpn. J. Appl. Phys. Lett.* **27**, L57 (1988).
- <sup>16</sup>S. Tsurumi, T. Iwata, Y. Tajima, and M. Hikita, *Jpn. J. Appl. Phys. Lett.* **27**, L80 (1988).